

# Nuchal Translucency Marker Detection Based on Artificial Neural Network and Measurement via Bidirectional Iteration Forward Propagation

LAI KHIN WEE, TOO YUEN MIN, ADEELA AROOJ, EKO SUPRIYANTO

Department of Clinical Science and Engineering  
Faculty of Health Science and Biomedical Engineering  
Universiti Teknologi Malaysia  
UTM Skudai, 81310 Johor  
MALAYSIA

[laikw2@gmail.com](mailto:laikw2@gmail.com) [eko@utm.my](mailto:eko@utm.my) <http://www.biomedical.utm.my>

*Abstract:* - Ultrasound screening is performed during early pregnancy for assessment of fetal viability and prenatal diagnosis of fetal chromosomal anomalies including measurement of nuchal translucency (NT) thickness. The drawback of current NT measurement technique is restricted with inter and intra-observer variability and inconsistency of results. Hence, we present an automated detection and measurement method for NT in this study. Artificial neural network was trained to locate the region of interest (ROI) that contains NT. The accuracy of the trained network was achieved at least 93.33 percent which promise an efficient method to recognize NT automatically. Border of NT layer was detected through automatic computerized algorithm to find the optimum thickness of the windowed region. Local measurements of intensity, edge strength and continuity were extracted and became the weighted terms for thickness calculation. Finding showed that this method is able to provide consistent and more objective results.

*Key-Words:* - nuchal translucency, ultrasound, fetal, pattern recognition, artificial neural network

## 1 Introduction

Recent studies show that fetal abnormalities can be detected through assessment of particular ultrasound markers such as nuchal translucency (NT), nasal bone, long bone biometry, maxillary length, cardiac echogenic focus and Doppler assessment of ductus venous [4] [23] [24]. So far, measurement of NT thickness in the first trimester of pregnancy has been proposed as the most powerful marker in the early screening for fetal abnormalities such as Trisomy 21, 18 and 13 [1]. An increased NT thickness that more than 2.5mm in between 11 and 13 weeks plus 6 days has also been associated with an increased risk of congenital heart diseases and genetic syndrome [7] [8] [9] [25].

The term nuchal translucency was coined by Nicolaides and colleagues to describe the collection of fluid that is normally present behind the neck of the first trimester fetus. Nicolaides wrote the term translucency encompasses both septated (cystic hygroma) and nonseptated lesions [21]. Nuchal Translucency is the subcutaneous fluid filled space between the back of the neck of a fetus and the overlying skin [4]. Normally it can be viewed in the ultrasound images for all fetuses during the first trimester of pregnancy [7]. By 1995, first large studies of NT confirmed that NT thickness can be reliably measured at 11-14 weeks, when combined with maternal age, can provide an effective means of screening Down syndrome. The importance of measuring NT as a screening tool can be evaluated from

the fact that all over Europe, America and UK, NT measurement is included in their prenatal screening programmes. According to National Institute of Health And Clinical Excellence (NICE) guideline the combined test, (NT, beta human chorionic gonadotrophins and pregnancy associated plasma protein-A) should be offered to screen Down Syndrome between 11 weeks and 13 weeks + 6 days to all pregnant women [22]. The NT thickness is measured as the maximum thickness of the translucent space in the sagittal view of fetus through the ultrasonic prenatal screening. The ability to achieve a reliable measurement of NT depends on proper training and adherence to a standard technique to achieve uniformity of results from different operators. However, measurement of NT by locating the sonogram callipers manually requires highly trained and experienced operators [10], and is therefore prone to errors, intra-observer and inter observer repeatability can be questioned [11]. Efforts have been made by numerous investigators worldwide to try to find an approach for boundary detection in ultrasonic NT images which is less reliant on human operators. As it is reducing the amount of human intervention, it will also reduce inter-observer and intra-observer variability. Moreover, it is expected to prevent the problem of drift in measurements over time in longitudinal studies.

Artificial neural networks have been widely applied in ultrasonic image processing chain for the tasks ranging from pattern recognition to identification,



## 2 Material and Methods

In this section, we describe the procedure of image acquisition, method of NT detection and measurement. The images of fetus with NT were obtained using KNOTRON (Sigma 330 Expert) ultrasound machine with a 3.5MHz convex transducer with freeze-frame capability. The Fig. 2 shows the block diagram of image acquisition from ultrasound machine to our developed hardware. Mid sagittal view of the fetal profile must be obtained by moving the transducer probe from side to side so that the inner edges of the two thin echogenic lines that border the NT layer is obtained [20]. The magnification of the image should be at least 75 percent zooming such that the head and thorax region occupy full screen of the image in the neutral position. The ultrasound gain setting remained unchanged throughout the entire study. The ultrasound images were obtained as the sequence of moving pictures. Still frame which is suitable for the proposed work was chosen.

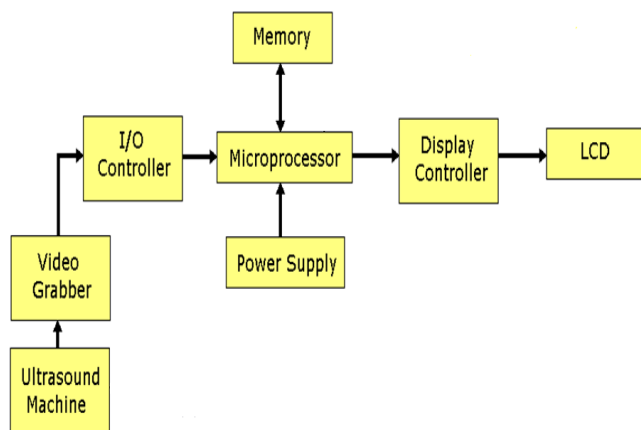


Fig. 2 Block diagram of image acquisition from ultrasound machine

In order to compute NT thickness, the region of interest (ROI) that encloses NT must be defined for reducing the undesired interference from the ultrasound image. The redundant information outside the defined region was discarded to minimize the errors during the measurement of NT afterwards. However, conventional image segmentation techniques are not applicable to ultrasound image processing due to its speckle noise and image artifacts. A wide variety of segmentation techniques have been considered and we proposed to use neural networks in our study. We used a multilayer feed forward neural network throughout this study.

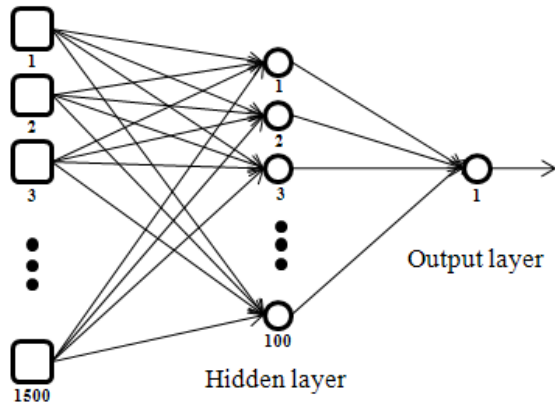
### 2.1 Architecture of neural network learning and feature extraction

ANN is a parallel distributed mainframe [5] that has a natural tendency for storing experiential information. A key benefit of neural networks is that a model of the system can be built from the available data. Image classification using neural networks is done by texture feature extraction and then applying the backward propagation algorithm. In this study, we used one of the common applied feed forward ANN architectures, which is multilayer perceptron (MLP) network containing one or more hidden layers. The function of neurons in the hidden layer is to arbitrate between the input and the output of the neural network. The input feature vector is fed into the source nodes in the input layer of the neural network. The neurons of the input layer constitute the input signals applied to the neuron in the hidden layers. The output of the hidden layer can be used as input for next hidden layer or output layer. The output layer produces the output result and terminates the neural computing process when it meets its target eventually. The main advantages of MLP compared to other neural model structures are that it is simple to implement and it can approximate any input/output map [6]. MLP consists of (a) an input layer with neurons representing input variables to the problem, (b) one or more hidden layers containing neuron(s) to help capture the nonlinearity in the system, and (c) an output layer with neuron(s) representing the dependent variable(s). We used the logistic function as an activation function  $f(x)$  for determining the output of neural network, as shown in equation 1 below.

$$f(x) = \frac{1}{1 + e^{-x}} \quad (1)$$

In this works, catalogue containing a total of 150 ultrasound fetal images with NT and without NT are vectorized into  $M \times N$  matrix respectively and fed as the input of neuron nodes in input layer for training purposes. The dimensional matrix  $M \times N$  can be fixed for an image of any size. In this study, the dimensional matrix is  $50 \times 30$  which produced 1500 elements of image feature vector. Therefore, we used multilayer perceptron network with 1500 input nodes, 100 hidden nodes and one output node, as illustrated in Fig. 3.

The value produced by the output neural node was used to calculate the probability of given image whether it contains a NT or not, and its value range between 0.9 and 0.1. When the output value of an ultrasound fetal images was exceeded, the set threshold was nearest to 0.9, the system classified the given image contains NT. Conversely, when the value is close to 0.1 or below the set threshold, the system classified the given image contains no NT.



Input layer

Fig. 3 Structural graph depicts the multilayer neural network used in this study. Numbers indicate the number of nodes.

During the training phases, we iteratively executed the back propagation learning algorithm for the training set and then produced the synaptic weight vectors that were applied to the neural network. The mean squared error (MSE) of the backward propagation is calculated using equation 2. Our developed NT detection model classified the location of NT by applying the final synaptic weight vectors to the multilayer neural network.

$$E_p = \frac{1}{2} \sum_{j=1}^{N_o} (t_{pj} - O_{pj})^2 \quad (2)$$

Where  $E_p$ : MSE,  $t_{pj}$ : target value for  $j_{th}$  output neuron,  $O_{pj}$ : actual output of  $j_{th}$  output neuron.  $N_o$ : total number of output neuron. Back-propagation is an essential to minimize the total network error by adjusting the weights. During this process, weight connecting neuron must be adjusted according to the general equation 3 and 4 as defined below:

$$\Delta w_{ji}^m = \eta \delta_j O_i + \alpha \Delta w_{ji}^{(m-1)} \quad (3)$$

$$w_{ij}^{(m+1)} = w_{ij}^{(m)} + \Delta w_{ij}^{(m)} \quad (4)$$

Where  $\eta$  is learning rate,  $\delta_{pj}$  is error signal and  $O_{pj}$  is output neuron. The adjustment of weight will be stopped when the MSE of the forward propagation is lower than the threshold value. During training, momentum value was fixed at 0.9, and learning rate was determined at level 1 on the hidden layer and 0.1 at the output layer. The training process was carried on for 10,000 epochs or until the cross-validation data's mean-squared error

(MSE), calculated by Equation 2, did not improve for 100 epochs to avoid over-fitting of the network. A plot of MSE versus the number of epoch is shown in Fig. 4. The training halted once the threshold is achieved at 2863 epochs. Descending graph shows that the weight is adjusted near to the target output. Now, the neural network is being well trained and can be tested using the actual data.

## 2.2 Neural network testing

For the network testing phase, neuron nodes in the input layer will be the centre of potential NT contained window  $C_{i,j}$ , where it can be computed through the convolution between a template of NT image  $NT_{i,j}$ , and sample ultrasound fetal images  $f_{i,j}$ .

$$C_{i,j} = f_{i,j} * NT_{i,j} \quad (5)$$

Fig. 5 illustrates the outcomes of convolution between sample ultrasound fetal images and NT template. The potential NT contained windows were vectorized into  $50 \times 30$  sized matrix  $V_k$ , where  $k$  is the number of  $C_{i,j}$ . The  $V_k$  is practiced within the trained network in order to identify the probability of each window, which is the calculated neuron in output layer. Maximum value of the neuron nodes in output layer, which was nearest to positive 0.9 was chosen as the final ROI. Fig. 6 shows the experimental result of ROI extraction by choosing the window with highest probability.

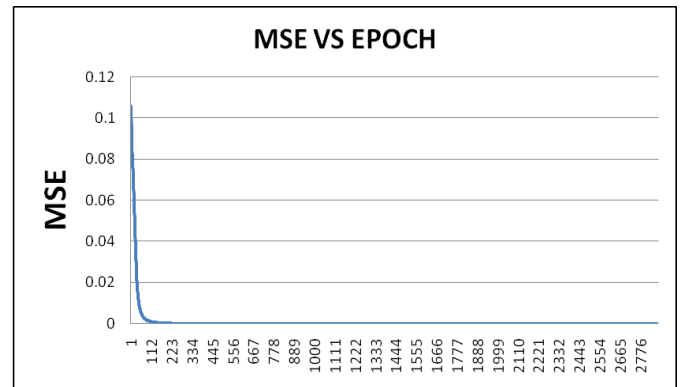


Fig. 4 MSE versus the number of epoch for network training.

In order to justify the performance of trained neural network, two different groups of testing images  $k_1$ ,  $k_2$  were used. Each groups of testing catalogue consisted of 30 numbers of ultrasound fetal images. The first group  $k_1$  were new registered images with nuchal translucency screening from a consecutive group of patients by using the same ultrasound scanner as the one used in training, where the second group of images  $k_2$  were randomly selected from Health Centre, Universiti Teknologi

Malaysia which contains no nuchal translucency in the images, Table 1 lists the performance of neural network on  $k_1$  and  $k_2$  groups of images. Simulations result shows

that the trained network capable achieving as high as accuracy about 93.33 percent and able to provide reliable and consistent findings.



Fig. 5 Location of centre potential NT window

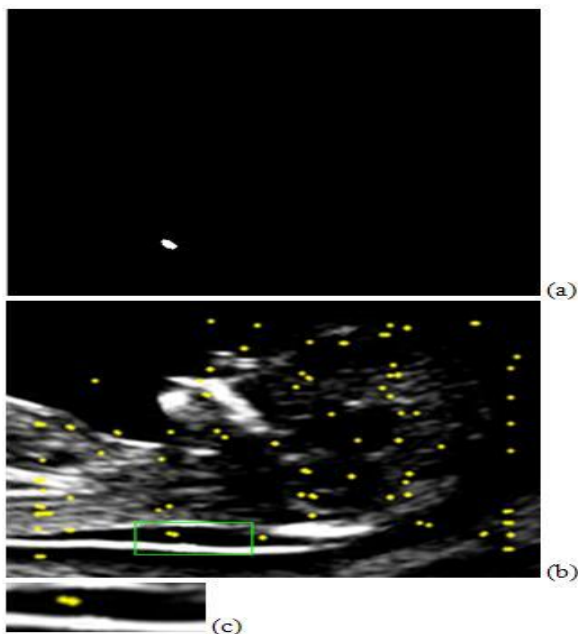


Fig. 6 Experimental result of ROI extraction. (a) The window with highest probability. (b) ROI on sample ultrasound image. (c) Resultant windowed NT region

**Table 1 – PERFORMANCE OF THE NEURAL NETWORK FOR NT RECOGNITION AND DETECTION**

Threshold	Group $k_1$	Group $k_2$	Accuracy
neural network output $> 0.85$	27 true-positive (TP)	1 false-positive (FP)	93.33%
neural network output $< 0.85$	3 false-negative (FN)	29 true-negative (TN)	
Total	30	30	

$$Accuracy = (TP + TN) / (TP + TN + FN + FP)$$

### 2.3 NT measurement

Conventional edge detection such as Sobel and Canny techniques has a drawback in NT measurement, as more than two echogenic lines will be mapped within the output image. In order to solve that problem, we had

applied our unique developed algorithm for NT edge detection, known as “Bidirectional Iterations Forward Propagations Method (BIFP)”. Let’s assume the acquired ROI is an  $M \times N$  rectangle, and then all possible borders  $T_N$  are considered as polylines with  $N$  nodes:

$$T_N = [p_1, p_2, \dots, p_{N-1}, p_N] \quad (6)$$

Where the pixels  $p_{N-1}$  and  $p_N$  are horizontal neighbors and  $N$  is the horizontal length of a contour line. The function of NT backbone  $b(r)$  is build according to reference points  $r$ , which are defined as follows:

$$r_{1,2} = \min [f(p_{1,N})] \quad (7)$$

The term  $f(p_{1,N})$  measures the intensity gradient and intensity of pixels along  $p_1$  and  $p_N$ , as shown in Fig. 7. Applied equation (7), the  $b(r)$  is formulated based on linear equation, as expressed follows:

$$y_j = \nabla b(r)x_i + r_1 \quad (i = 1, \dots, N) \quad (j = r_1, \dots, r_2) \quad (8)$$

$$\nabla b(r) = \frac{|r1 - r2|}{N} \quad (9)$$

Where  $x_i$  and  $y_j$  are the coordinate along this linear equation. Fig. 8 illustrates the linear equation coincide with both reference points  $r_1$  and  $r_2$ . The bidirectional forward propagation tracking process is used to scan through the NT edges of upper and lower boundaries within the  $M \times N$  ROI referring to  $b(r)$ , and stored in the array of  $T_{N1}, T_{N2}$ , as shown below:

$$T_{N1} = \max [\nabla \text{ROI} (x_i, y_j - d_{1i})] \quad (10)$$

$$T_{N2} = \max [\nabla \text{ROI} (x_i, y_j + d_{2i})] \quad (11)$$

Where  $d_{1i}$  and  $d_{2i}$  are y-coordinates for maximum intensity gradient of both upper and lower border. The NT thickness was taken along every five pixels of polylines  $T_{N1}$  and  $T_{N2}$ . The maximum thickness of the subcutaneous translucency between skin and the soft tissue overlying the cervical spine should be measured. Therefore, the largest thickness is recorded as the NT measurement and calibrated with scale of ultrasound image to get the exact thickness in millimeter, as shown in Fig. 9.

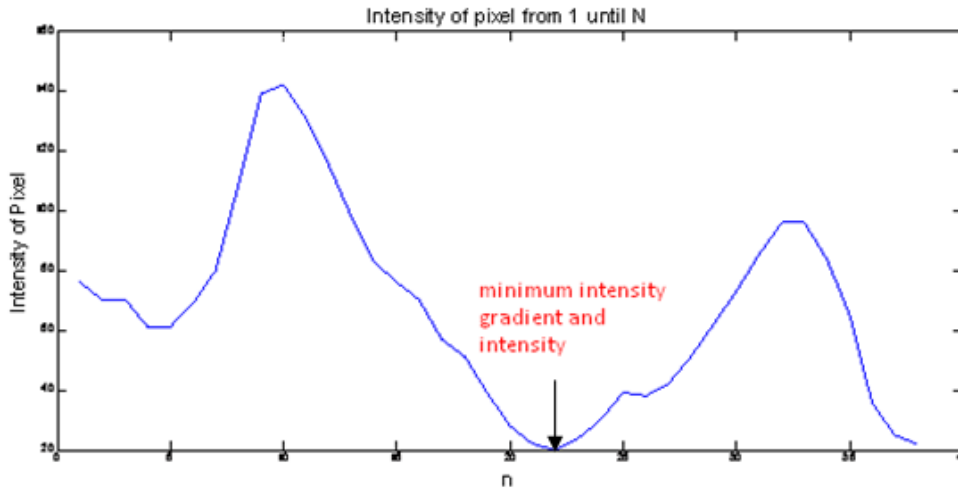


Fig. 7 Intensity gradients and intensity of pixels along  $p_1$  and  $p_N$ .

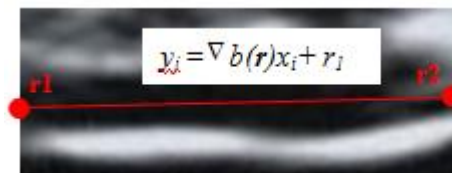


Fig. 8 Formation of NT backbone  $b(r)$  using both reference points  $r_1$  and  $r_2$ .

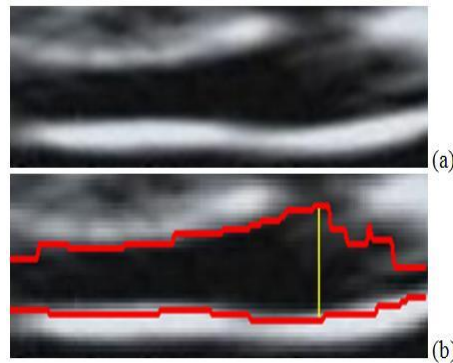


Fig. 9 Experimental result of maximum thickness NT measurement (a) Sample original image (b) Edge tracking and NT measurement.

### 3 Result and Analysis

The result of this study is divided into two parts. The first parts of finding are the result of ultrasonic NT region of interest recognition and detection using trained network. The second part is the automated measurement of NT using the state of the art BIFP computerized method.

In order to access the performance and usefulness of the trained and validated system in a real application, a thorough evaluation of the method was carried out at the Medical Electronics Research Laboratory, Universiti Teknologi Malaysia, Malaysia. We ran the algorithm on a set of ultrasound images, with 640 x 480 sized ultrasound fetus images obtained by transabdominal ultrasonography. New images were registered from a consecutive group of patients and control subjects ( $n = 30$ ) using the same ultrasound scanner as the one used in training.

Table 1 lists the performance of trained neural network on two different groups of testing samples. The accuracy of the neural network for detecting NT was 93.33 percent (56 of 60). Based on equations 12, 13, 14 and 15 the calculated sensitivity was 90 percent (27 of 30), the specificity was 96.67 percent (29 of 30), the positive predictive value was 96.43 (27 of 28) and the negative predictive value was 90.63 (29 of 32). These results indicate the developed diagnostic model making well recognition and detection of NT.

$$Sensitivity = TP / (TP + FN) \quad (12)$$

$$Specificity = TN / (TN + FP) \quad (13)$$

$$Positive Predictive Value = TP / (TP + FP) \quad (14)$$

$$Negative Predictive Value = TN / (TN + FN) \quad (15)$$

Fig. 11 shows part of our experimental results using sample patients' data and the obtained findings

demonstrated that the state of the art of BIFP computerized method is able to produce accurate border in most of the samples. Using the Sobel and Canny edge detectors' results in discrete borders is not correctly matched to the borders, whereas our method extracts continuous borders accurately in Fig. 10. In cases of extremely poor in contrast and resolution of ultrasound images as shown in the last two samples (j) and (k) in Fig. 11, miss calculation and discontinuity border detection are hardly to be avoided since BIFP heavily dependent on the weighted terms including intensity gradient and edge strength.

For quantitative analysis, we calculated their means and standard deviations ( $SD$ ) between automatic and manual measurements for the maximum NT thickness. The covariance ( $COV$ ) of respective methods was then calculated according to formula below:

$$cov(X, Y) = \sum_{i=1}^N \frac{(xi - \bar{x})(yi - \bar{y})}{N} \quad (16)$$

Where  $X$ : manual method,  $Y$ : automated method,  $N$ : total number of sample,  $\bar{x}$  and  $\bar{y}$  are mean of each method.

$$corr = \frac{cov(X, Y)}{\sqrt{var(X) \times var(Y)}} \quad (17)$$

The correlation for two analyzing methods was least 0.98 for all of the measurements using Equation 17. Table 2 presents a comparison of the measures from the manual and automated system respectively.











